PCCP

PAPER

Cite this: *Phys. Chem. Chem. Phys.*, 2015, **17**, 13257

Fluorinated graphene dielectric films obtained from functionalized graphene suspension: preparation and properties

N. A. Nebogatikova,*[a] I. V. Antonova,*[ab] V. Ya. Prinz,[a] I. I. Kurkina,[c] V. I. Vdovin,[a] G. N. Aleksandrov,[c] V. B. Timofeev,[c] S. A. Smagulova,[c] E. R. Zakirov[a] and V. G. Kesler[a]

Received 14th October 2014,
Accepted 14th April 2015

DOI: 10.1039/c4cp04646c

www.rsc.org/pccp

In the present study, we have examined the interaction between a suspension of graphene in dimethylformamide and an aqueous solution of hydrofluoric acid, which was found to result in partial fluorination of suspension flakes. A considerable decrease in the thickness and lateral size of the graphene flakes (up to 1–5 monolayers in thickness and 100–300 nm in diameter) with increasing duration of fluorination treatment is found to be accompanied by a simultaneous transition of the flakes from the conducting to the insulating state. Smooth and uniform insulating films with a roughness of ~2 nm and thicknesses down to 20 nm were deposited from the suspension on silicon. The electrical and structural properties of the films suggest their use as insulating elements in thin-film nano- and microelectronic device structures. In particular, it was found that the films prepared from the fluorinated suspension display rather high breakdown voltages (field strength of (1–3) × 10^6 V cm^{-1}), ultralow densities of charges in the film and at the interface with the silicon substrate in metal–insulator–semiconductor structures (~(1–5) × 10^{10} cm^{-2}). Such excellent characteristics of the dielectric film can be compared only to well-developed SiO_2 layers. The films from the fluorinated suspension are cheap, practically feasible and easy to produce.

Introduction

Graphene and graphene-based materials have attracted huge practical and theoretical interest of many researchers.[1] The possibility to create lateral and vertical quantum structures, as well as to controllably tune the properties of such structures, is just one reason for studying graphene and obtaining, by means of chemical modification, graphene-based materials with new promising properties.[1–3] The bandgap opening in the energy spectrum of graphene is a most important and called-for modification of this material. Another important problem in graphene functionalization is the search for means that would allow control of material parameters of graphene and its derivatives.

The most widely known chemical derivatives of graphene are fluorinated graphene, hydrogenated graphene, and oxidized graphene. All those materials are high-resistivity or dielectric materials with bandgap energy in excess of 3 eV. As it was shown in a number of studies, the above materials show different stabilities of their properties.[4–8] The most stable material (in terms of thermal and time stability) is fluorinated graphene,[5] hydrogenated and oxidized graphenes being less stable derivatives.[4,9] On the other hand, the possibility of restoration of the initial properties of materials makes chemically modified graphene derivatives attractive for use in device structures.

For chemical modification of graphene aimed at obtaining fluorinated graphene, treatment of the material in a gaseous atmosphere or plasma is most frequently used. In all cases, favorable conditions for the reaction of graphene with fluorine involve high temperatures and pressures, and also the use of toxic substances, both circumstances making the fluorination process a difficult technological task.[4–8] The mentioned technological problems restrict the use of fluorinated graphene. Generally, large-scaled preparation of fluorographene or fluorinated graphene with a possibility to control the fluorination degree remains a great challenge. Easy-operating, highly scalable and low-cost approaches were reported for the preparation of fluorographene [for instance, ref. 10]. Earlier, we developed a simple and easy process for graphene fluorination at room temperature and atmospheric pressure in an aqueous solution of hydrofluoric acid (HF)[11,12] which proved to be a process offering a possibility to manage the fluorination degree of graphene and few-layer graphene sheets.

[a] *Rzhanov Institute of Semiconductor Physics, Russian Academy of Science, Siberian Division, Acad. Lavrent'ev Avenue, 13., 630090, Novosibirsk, Russian Federation. E-mail: nadonebo@gmail.com*
[b] *Novosibirsk State University, Pirogov Street, 2., 630090, Novosibirsk, Russian Federation. E-mail: antonova@isp.nsc.ru*
[c] *Ammosov North-Eastern Federal University, Belinskii Street, 58., 677000, Yakutsk, Russian Federation*

Nowadays, the methods for obtaining graphene include electrostatic or mechanical cleaving of graphite,[13,14] growth of graphene layers by chemical vapor deposition,[2,15] and chemical exfoliation of graphite (preparation of suspensions).[16,17] The approach using the preparation of graphene suspensions is the cheapest method for obtaining graphene and producing large-area graphene films; yet, such films usually show only a limited quality. One of the main problems here is to achieve splitting of graphite into monolayers without using chemical oxidation, and with a demand for reducing such suspensions or suspension-based films.[16,17] Very often, the obtained graphene suspensions contain particles in the form of graphite flakes several ten nanometers thick. Fluorination of suspensions was implemented for graphene oxide at elevated temperatures and pressures as well; as a result, oxyfluorographene suspensions were obtained.[3,7,18]

The purpose of the present work was to apply our new approach to graphene fluorination (treatment in aqueous solution of HF[11,12,19]) of graphene suspensions, and study the interaction of graphene suspensions with aqueous solutions of hydrofluoric acid. This study aimed at structural and chemical modification of suspension flakes, obtaining fluorinated graphene suspensions with various fluorination degrees, and formation and characterization of films from these suspensions. In the course of the fluorination procedure, we have discovered an unexpected phenomenon that consisted of additional splitting of suspension flakes into much thinner and finer elements in comparison with initial flakes. This phenomenon has allowed us to form uniform and thin large-area dielectric films. It was found that thin films (thickness 100–20 nm, roughness $\sim$2 nm) obtained from a fluorinated graphene suspension offer many useful dielectric material properties; namely, and, first of all, they exhibit high breakdown voltages and very low densities of charges in the film and at the interface with silicon in metal–insulator–semiconductor structures ($\sim 5 \times 10^{10}$ cm^{-2}). Both properties make such films promising candidates for use as insulating elements in thin-film device structures.

Experimental methods for formation, modification and characterization of graphene suspension

The starting material was a graphene suspension that was obtained by a standard procedure described in ref. 5, 16 and 17. The main stages in the preparation of the suspension were the following: mechanical crushing of natural graphite, dimethylformamide (DMF) intercalation, ultrasonic treatment intended for splitting the intercalated particles, and centrifugation intended for the removal of non-split graphite particles. In preparation of the suspension, the natural graphite was turned into particles with characteristic sizes of 1 to 2 μm (length and width) and up to 20–70 nm (thickness).

After the graphene suspension was obtained, it was subjected to a fluorination procedure. To this end, equal volumes of the graphene suspension and a 5% solution of hydrofluoric acid (HF) in water were mixed together. Periodically, some portions of the suspension were used for the study and preparation of films. The substrates for films were silicon (Si) wafers. During deposition of the films, the native oxide was removed from the surface of silicon by hydrofluoric acid present in the solution. The deposited films were dried and rinsed with deionized water for removing the residual hydrofluoric acid and the organic component of the suspension, and then they were subjected to a second drying treatment for water removal.

The properties of the films formed on silicon substrates were studied using the following experimental techniques: scanning electron microscopy (SEM), Raman scattering spectroscopy (RSS), X-ray photoelectron spectroscopy (XPS), atomic force microscopy (AFM), and measurement of capacitance–voltage and current–voltage characteristics. For acquiring AFM images of the film and substrate surfaces and for determining the film thickness, a Solver PRO NT-MDT scanning microscope was used. The measurements were performed in both contact and semi-contact mode. Raman spectra were recorded at room temperature, the excitation wavelength being 514.5 nm (2.41 eV argon ion laser). In order to avoid the heating of samples with laser-emitted radiation, the laser beam power was decreased to 2–3 mW. The spectra were recorded using an NT MDT Nanolaboratory INTEGRA Spectra spectrometer. SEM images were acquired using a JEOLJSM-7800F scanning electron microscope with the energy of primary electrons equal to 2 keV. The structural features of the sample(s) were examined by transmission electron microscopy (TEM, JEM-2200FS, 200 kV accelerating voltage). For measuring XPS spectra, an SSC Riber facility (Surface Science Centre Riber) was used. The measured XPS spectra permitted studying the chemical composition of obtained films. Fourier transform infrared (FTIR) absorbance spectra were recorded using a Varian 7000 FTIR spectrometer. Sixteen scans of each spectrum were taken using a range of 4000–550 cm^{-1} at a resolution of 8 cm^{-1}. For measuring capacitance–voltage and current–voltage characteristics, an E7-20 immitance meter and a Keithley picoamperemeter (model 6485) were used. The electrical contacts to the films were prepared by sputtering Au onto the film surface, the contact surface area being 0.5 mm^2. In this way, a set of vertical metal–insulator–semiconductor (MIS) Au/fluorinated graphene/Si structures was obtained.

Structure of fluorinated graphene films with various fluorination degrees

Films were prepared by means of pouring droplets of suspension on the silicon substrate with drying, rinsing in deionized water for removing the residual hydrofluoric acid and the organic component of the suspension, and a second drying treatment for water removal. We have to notice that addition of an aqueous solution of HF to a suspension changed the wettability of the silicon substrates with respect to suspension droplets; the fluorinated suspension easily spread over the surface of the substrate to form a thin continuous film.

By means of scanning electron microscopy and atomic force microscopy, we showed that the characteristic particle sizes in

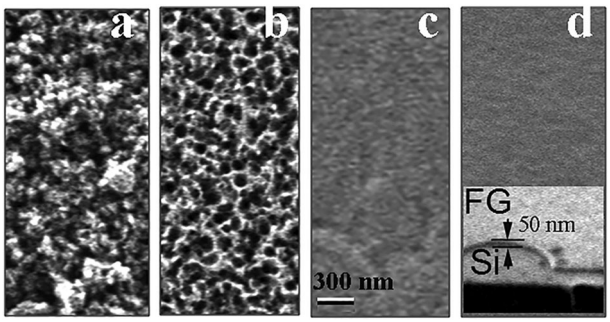

Fig. 1 SEM images of the surface of films fluorinated in the aqueous solution of HF for different times. The scales in the images are identical. (a) Pristine (non-fluorinated) film; (b–d) films fluorinated, respectively, for 2, 10, and 40 days. The inset in (d) shows an image of an edge of the film taken at the 45° angle to the surface; the film thickness indicated in the figure was evaluated with allowance for measurement geometry.

the formed films and the thicknesses of the films depended on the time duration for which the suspension was treated in the aqueous solution of HF. Fig. 1a–d presents scanning microscope images that prove that treatments of suspensions in an aqueous solution of HF led to improved uniformity of the surface of the obtained films and relief reduction on the film surface. The thickness of the films formed on the surface of silicon from droplets containing identical amounts of suspension decreased with increasing treatment duration, after 25 days of fluorination treatment, 150 to 100 nm thick films (respectively, at the center and the periphery of the sample) were obtained, whereas after 40 days of fluorination treatment the film thickness decreased to 80–50 nm (see the inset of Fig. 1d). The minimal thickness of the obtained continuous films was 20 nm. The typical thickness of films treated for 60–70 days was ~50–40 nm.

AFM images of the film surface acquired after fluorination are shown in Fig. 2. Note the additional splitting of graphene flakes in the suspension that occurred during the treatment (see Fig. 2a and b). One split off layer can be seen on each flake in Fig. 2a after 4 days of treatment, and two split off layers can be seen on each flake shown in Fig. 2b after 10 days of treatment. A comparison between the lateral and vertical sizes of the particles in Fig. 2a and c shows that those sizes decreased with increasing duration of the treatment in the aqueous

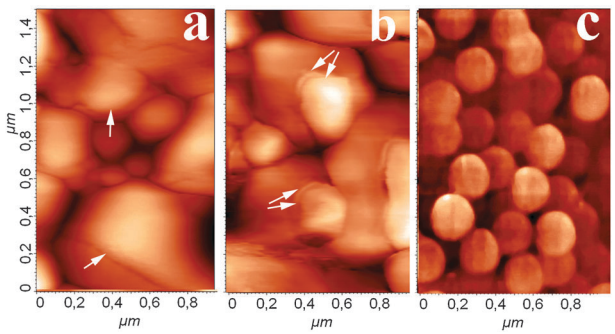

Fig. 2 AFM images of film surfaces. The films were obtained using suspensions of various fluorination degrees. (a–c) 4, 10 and 70 days of fluorination treatment, respectively. The splitting layers are shown with arrays.

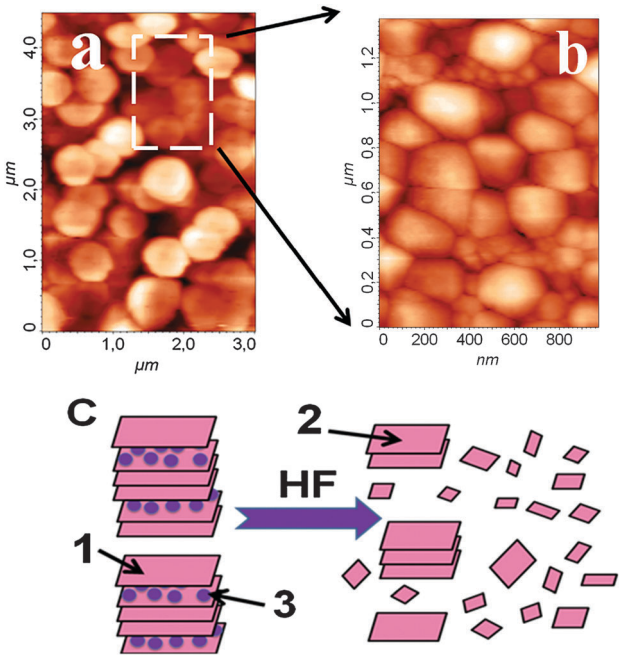

Fig. 3 AFM images of the surface of a film having been treated in the aqueous solution of HF for 60 days. (a) Image acquired at a lower magnification showing only large-scale particles. (b) Image showing large and fine fluorographene nanosheets. (c) A sketch illustrating the additional splitting of initial flakes and their fractionation into finer flakes that occurred during treatment of a suspension with an aqueous solution of hydrofluoric acid (1 – initial particle, 2 – split of partially fluorinated flakes, and 3 – intercalated DMF layer).

solution of HF. For better visualization of the processes occurring during the treatment of the suspension, Fig. 3a and b shows images of films at different scales. It is seen that, in the suspension, particles of two characteristic sizes, 200 to 400 nm and 20 to 50 nm, were present. The latter observation points to the fractionation of initial particles into finer particles (for more details, see Discussion).

The obtained data on the lateral sizes and thicknesses of the large-scale flakes are shown in Fig. 4. The minimal sizes of these flakes after 80–120 days of fluorination were found to be equal to 100 to 300 nm (diameter) and 0.5 to 2.0 nm (thickness). Thus, the processes leading to the splitting and fragmentation of large particles into finer particles get decelerated or ceased over rather long times of treatment. The finest flakes had characteristic sizes of 20 to 50 nm, with their thickness exhibiting no noticeable dependence on the treatment duration and their concentration increasing with increasing duration of fluorination treatment.

Fig. 5 displays the TEM images of one of the films. Round flakes are clearly seen in these images with relatively large (20–30 nm) and small (5–10 nm) sizes. These images are in good agreement with the AFM data and the suggested model (Fig. 2 and 3).

Evidences for the fluorination reaction of graphene flakes

One main evidence of fluorination is the transition from conductive to insulation properties of the films formed from

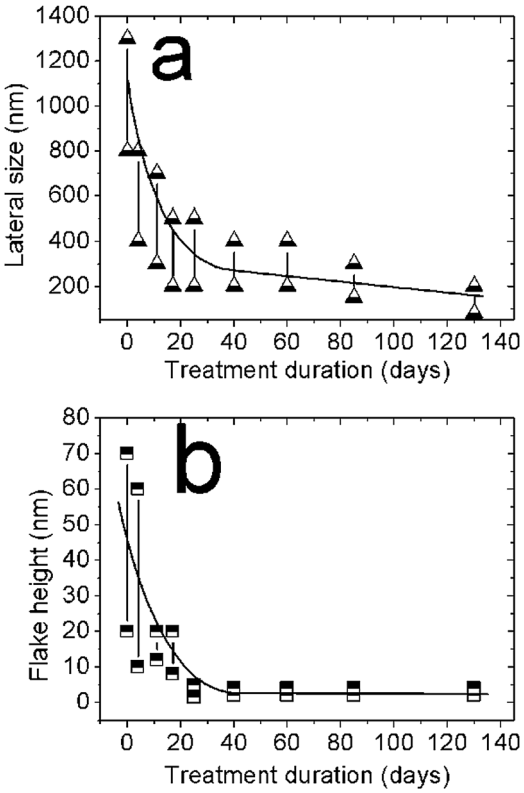

Fig. 4 Lateral sizes (a) and thickness (b) of suspension particles *versus* the duration of HF treatment. The solid line is added to the plots to facilitate data comprehension.

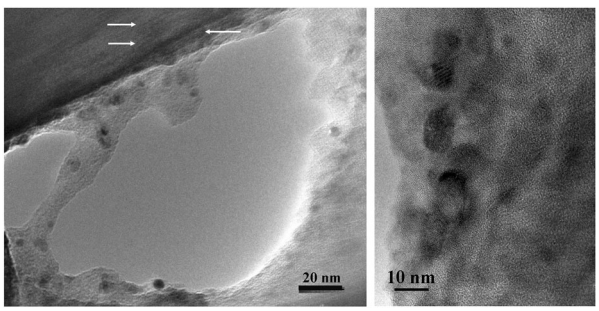

Fig. 5 TEM images of films treated in the aqueous solution of HF for 70 days in the multi-beam diffraction (left) and high resolution electron microscopy (right) modes. Arrows are marked for some of the relatively large flakes.

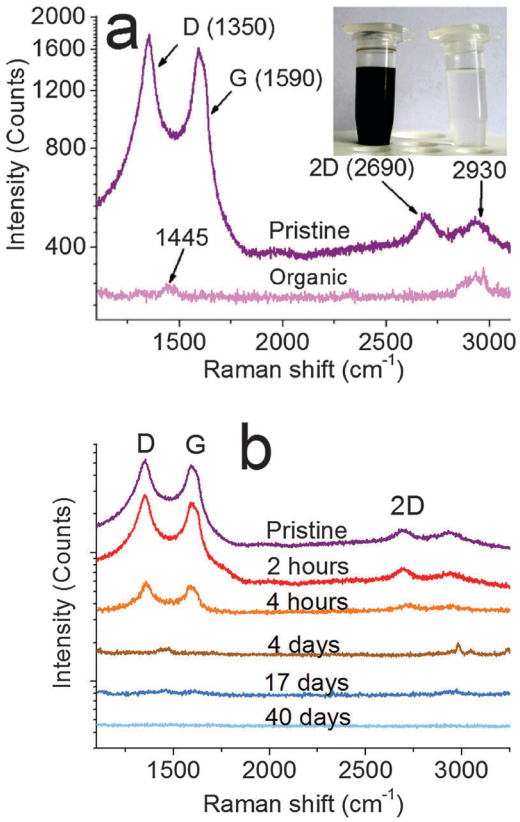

Fig. 6 (a) Typical Raman spectra of a pristine suspension and the organic solution component in the suspension. (b) Evolution of Raman spectra of pristine fluorinated films with the duration of HF treatment. The inset in Fig. 5a shows the vessels with non-fluorinated and fluorinated suspensions (left and right vessels, respectively).

the suspension treated in the aqueous solution of HF for more than 25 days. In detail, the insulated properties of films will be given in the next section.

During treatment of a graphene suspension in an aqueous solution of HF, color changes visible to the naked eye occurred in the suspension. The inset in Fig. 6a shows a photo of two vessels, one (left) vessel containing graphene suspension prior to fluorination treatment, and the other (right) vessel with graphene suspension after the treatment. The change in suspension color was not due to sedimentation of a precipitate in the vessel since the color could not be restored by stirring the suspension. The change in suspension color observed on fluorination, in addition to reduced sizes of suspension particles, could be due to the formation of fluorographene. Indeed, it is known that fluorinated graphene is a white substance with a bandgap width of 3.2 eV.[5,18]

The gradual emergence of fluorinated graphene properties could be traced in the measured Raman spectra of our samples. Prior to analyzing the effect of fluorination on the spectra, we would like to describe the Raman features observed in the spectra of pristine (non-fluorinated) samples. The known Raman features of graphene (graphite) are a weak D peak (1350 cm^{-1}), a G peak (1590 cm^{-1}), and a 2D peak (2690 cm^{-1}). The Raman spectra of our samples contained a considerable contribution of the D peak due to flake edges, so that the amplitude of the G peak was comparable with that of the D peak, the latter peak being forbidden in ideal graphene and graphite lattices. The emergence of a D peak in the Raman spectra of graphene films is due to sp^3-hybridized carbon atoms present in the films (carbon atoms with dangling bonds or atoms with chemical bonds outside the graphene sheet). Also, the Raman spectra additionally contained peaks due to DMF and its derivatives. In the Raman spectra of our samples, those features were 1445 and 2930 cm^{-1} peaks due to differently deformed DMF molecules. The 1445 cm^{-1} peak is known to be due to the asymmetric bending of carbon–hydrogen bonds in the CH_2 "molecule", and the 2930 cm^{-1}

peak, due to the stretching vibrations of such bonds.[20,21] Moreover, the 1445 and 2930 cm^{-1} peaks were observed for molecules containing CH_2 fragments. Note that, for the C–N bond, a peak at around 1430 cm^{-1} can also be expected.[22] It is worth noting that no such peaks were observed in graphene and few-layer graphene films obtained by electrostatic exfoliation of graphite and in graphene and few-layer graphene films grown by chemical vapor deposition (CVD).[11,12]

Raman spectra recorded on the films obtained from suspensions fluorinated for different times are shown in Fig. 6b. It is seen that an increased duration of treatment of the suspension in the aqueous solution of HF resulted in a decreased intensity of peaks in Raman spectra, this effect is typical for fluorination of graphene.[5,18] The latter modification of Raman spectra was due to the opening of a bandgap in fluorographene (~3.0–3.5 eV), resulting in the excitation energy (2.41 eV) no longer being sufficient for the occurrence of band-to-band electron transitions. The gradual decrease of the amplitude of Raman peaks implies that the fluorination degree of the films gradually increased with the treatment duration.

A concomitant weakening of DMF-induced peaks at 1445 and 2930 cm^{-1} also deserves mention. Most probably, this observation means that the solution of HF penetrated inside the few-layer graphene films along the DMF intercalation planes. The presence of water in the solution promoted the decomposition of DMF into constituents and the release of heat during decomposition. Owing to the heat released during DMF decomposition the fluorination reaction was promoted. Fluorination of graphene led to the local modification of carbon atom hybridization, change in the lattice constant, emergence of mechanical stress, and change in the reactivity of the immediate surroundings. Graphene fluorination also led to a local change in the graphene layer wettability. Those changes led to the promotion of the penetration of the HF-containing solution into the graphene films, the spreading of fluorination reaction inside the flakes, and the additional splitting of flakes.

A common spectrum and carbon and fluorine related XPS spectra are shown in Fig. 7. A signal from fluorine F 1s was detected in the energy region of 687.7 eV in the spectra of the obtained HF-treated films. Such a position of the peak corresponds to sp^3 hybridized chemically bound fluorine ions[18,23,24] and the bond has a covalent character.[5,25] For comparison, the position of the line of fluorine at 685.5 eV means that fluorine ions are bound to carbon by an ionic bond when carbon has sp^2 hybridization. The energy position and shape of the peaks are indicative of partial fluorination of suspension particles (in the material, there remain carbon atoms not bound to fluorine).[26] Carbon C 1s peak decomposition is given in Fig. 7c–e. The appearance of peaks attributed to C–CF (285.6 eV), $C–CF_2$ (286.9 eV) and C–F (289.3) is observed.[5,7,27] An increase in the HF treatment time up to 60–70 days leads to the shift of the C 1s peak position from 284.5 eV (C–C) to 285.6 eV (C–CF). The ratio between the areas under the peaks, due to carbon and fluorine, of films treated in the HF-containing solution for 25 days (with allowance for different sensitivities of XPS to the two elements) corresponds to the formula C_2F. Si- and O-related line intensity corresponds to native SiO_2 on the Si substrate with a thickness

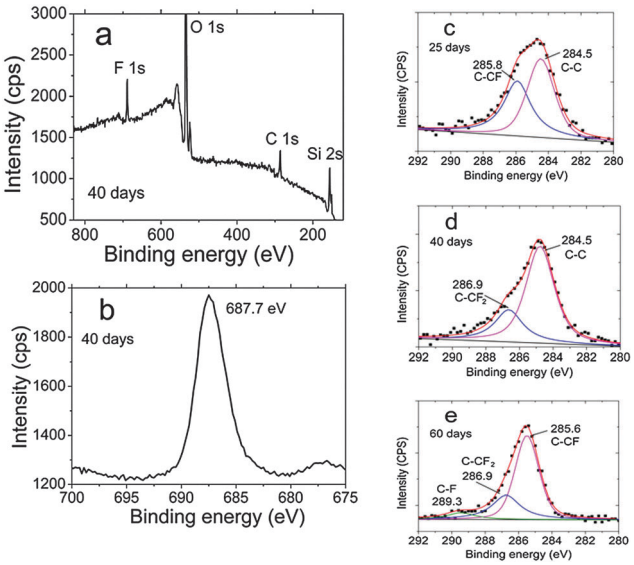

Fig. 7 (a) XPS spectra of the film formed from suspension treated in the aqueous solution of HF for 40 days and (b) fluorine related XPS spectrum of the same film. F 1s spectra of all films had the same position. (c–e) Carbon related (C 1s) XPS spectra (points) of the films treated in the aqueous solution of HF for 25, 40, and 60 days, respectively. Fitting of XPS C 1s spectra (curves) with components mentioned in the figures.

of 1–4 nm. The observation of the Si substrate with native SiO_2 on the surface was correlated with the fact that the tested area was larger than the film size.

The FTIR spectra obtained in the absorption mode for a few fluorinated films are given in Fig. 8. Strong IR bands with maxima at 1107, 1166 and 1230 cm^{-1} are clearly seen. When the fluorine atom is connected *via* sp^3-hybridization, the C–F bond is considered as covalent bonding, with the stretching vibration absorption corresponding to the peak at 1221 cm^{-1} (ref. 27) or 1260 cm^{-1}.[28] For fluorographene exfoliated by *N*-methyl-2-pyrrolidone, peaks at 1212 and 1084 cm^{-1} were observed corresponding to the stretching vibration of the C–F covalent bonds and the semi-ionic stretching vibration of C–F bonds, respectively.[29] The studies of FTIR spectra with an increasing fluorination time have revealed that the absorption band at

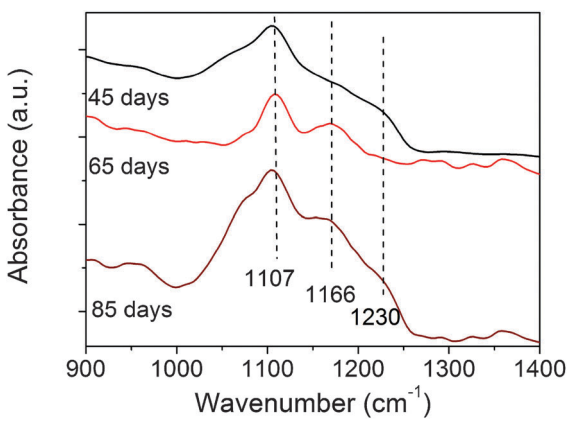

Fig. 8 FTIR spectra of some fluorinated films. Time duration of the treatment is given in the figure as a parameter.

1112 cm^{-1} gradually shifts to 1211 cm^{-1}.[30] The modes observed in the present study are suggested to correspond to those evaluated with the fluorination time of the C–F bond.

The stability of the electrical properties of the film after thermal annealing in the temperature range 100–350 °C allows us to state that oxidation does not occur during HF treatment.

A good chemical stability of the obtained films is noteworthy. Additional treatments of structures with films on their surface in water, acetone and toluene were performed; such treatments caused no noticeable changes in the properties of fluorinated films.

Dielectric properties of films

For measuring the capacitance–voltage characteristics, the obtained fluorographene films were provided with electrical contacts; such contacts were obtained by sputtering Au onto the film surface. The photograph of contacts and a sketch of the obtained vertical MIS structures are presented in Fig. 9a and in the insets of the figure.

The films prepared from the non-fluorinated suspension (0 days of fluorination treatment) were conducting films. After HF treatment of ~25 days, the films proved to be dielectric films. The capacitance–voltage characteristics of an MIS structure measured at a frequency of 1 MHz with the graphene film fluorinated for 40 and 60 days are shown in Fig. 9. After 40 days of fluorination treatment, the maximal electric-field strength that could be withstood by the films, or the breakdown field strength, was ~1.2×10^6 V cm^{-1}. Increasing the duration of fluorination treatment resulted in a moderate increase of the breakdown voltage (within the range 1.2×10^6 to 3×10^3 V cm^{-1}). The values of the dielectric constant ε of the films *versus* the duration of fluorination treatment are shown in the inset of Fig. 9b. For calculating those values, the maximal capacitance (plateau) at capacitance–voltage characteristics C_m and film thickness d obtained by SEM and AFM were used. The well-known equation for a parallel-plate capacitor can be written as $C_m = A\varepsilon_0\varepsilon/d$, where ε_0 is the permittivity of the vacuum and A is the surface area of the contact. It is seen that the magnitude of ε gradually approaches a value of 1.1. In ref. 31 similar measurements performed on multilayer structures (up to 10 monolayers) of fluorographene have yielded a value ε = 1.1 for the dielectric constant. The graphite dielectric constant is known to be equal to 10–15. A number of models have been proposed and used for predicting the effects of second phases on the dielectric properties of the composites.[32] A change in the dielectric constant of a composite, with respect to the filler concentration, can be explained by well-established laws such as the Bruggeman self-consistent effective medium approximation,[33] the Maxwell–Garnett equation[34] and other models.[32,35] We considered graphene inclusions as fillers and fluorographene as a matrix. From the value of the effective dielectric constant of partially fluorinated films, the relative degree of fluorination of suspension particles could be determined. For this purpose, in the present study, we used the relation,[32,35]

$$\frac{\varepsilon_{exp} - \varepsilon_{FG}}{\varepsilon_{exp} + 2\varepsilon_{FG}} = \nu \times \frac{\varepsilon_G - \varepsilon_{FG}}{\varepsilon_G + 2\varepsilon_{FG}}, \quad (1)$$

where ε_{exp} is the experimentally evaluated dielectric constant of the partially fluorinated film, ε_G and ε_{FG} are graphene and fluorographene dielectric constants, respectively, and ν is the graphene volume fraction. The degree of graphene fluorination was determined using $(1 - \nu)$. The obtained dependence for the fluorination degree is shown in Fig. 9b.

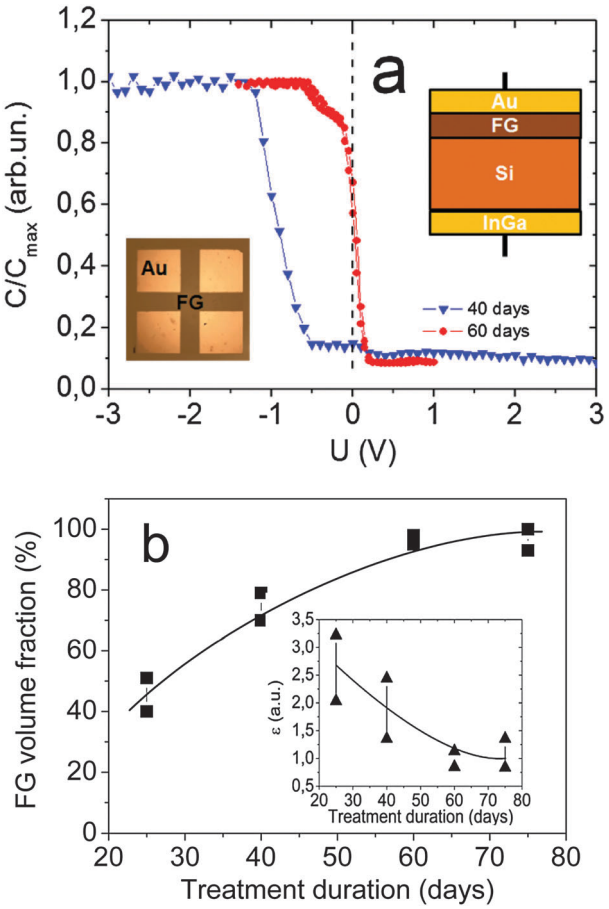

Fig. 9 (a) Capacitance–voltage characteristics of two Au–fluorographene–Si–InGa structures measured at 1 MHz frequency. The fluorographene films were obtained from suspension using fluorination procedures that lasted for 40 and 60 days. The inset in the right part of the figure shows a schematic representation of the measured structure (Me are the metal contacts (Au on the fluorographene film and InGa alloy on the silicon substrate), Si is the silicon substrate, and FG is the fluorographene film). The rate of voltage sweep in measuring the capacitance–voltage characteristics was 0.03 V s^{-1}. The capacitance–voltage characteristic of the 60 day film was recorded by sweeping the voltage in two opposite directions; the data are indicative of no hysteresis. The inset in the left part of the figure shows the image of the film on the surface of silicon with Au contacts. The size of the square is 0.7 mm. (b) Film fluorination degree *versus* the duration of fluorination treatment in the solution of HF in water. The inset in Fig. 9b shows the value of dielectric constant ε *versus* the duration of the fluorination treatment.

The above relation is valid for gradually proceeding graphene fluorination in the fluorographene matrix with volume type of fillers. In the case of a high aspect ratio of graphene fillers (large graphene flakes), the dielectric constant of the composite had strongly changed already for a low nanosheet volume fraction (1–2%).[36] In our case, the graphene fillers are suggested to have a small size and a low aspect ratio of graphene or few-layer graphene flakes. This suggestion is based on the data in Fig. 8 and the appearance of photoluminescence from the film in the

visible region which allows us to estimate the size of graphene fillers to be $\leq$10 nm.

To evaluate the potential offered by the films under study as dielectric layers in thin-film device structures, we performed an analysis of the capacitance–voltage characteristics of MIS structures with such films with the aim to evaluate the fixed charge density in the film and the density of interface states at the film/Si substrate interface. The density of the fixed charge in the film Q_f was evaluated from the flat-band voltage as determined from the capacitance–voltage characteristics. The density of interface states at the interface with silicon D_{it} was determined from the difference between the charge Q_f and the charge Q_{mg} that was determined from the bias voltage at which the Fermi level took position in the middle of the bandgap of the semiconductor substrate. It can be recalled that the fluorinated graphene film was applied onto a silicon surface free of native oxide. For films fluorinated for 25 days, the densities Q_f and D_{it} proved to be, respectively, $(4–6) \times 10^{11}$ cm^{-2} and $(3–5) \times 10^{10}$ cm^{-2}. On increasing the duration of fluorination treatment, the densities Q_f and D_{it} were found to decrease in value. In a film that was fluorinated for 65 days, the densities Q_f and D_{it} were found to be as low as $\sim 5 \times 10^{10}$ cm^{-2} and $(1.5–3) \times 10^{10}$ cm^{-2}, respectively; this finding proves that the quality of the obtained dielectric films can be improved by increasing the treatment duration. On the whole, the obtained values proved to be much lower than the values of Q_f and D_{it} typical for many dielectric coatings used in nano- and microelectronics (for more details, see Discussion).

Discussion

The experimental data obtained in the present study using various characterization techniques allow the following conclusions to be drawn: (1) evidence for a fluorination reaction proceeding in examined graphene suspensions was obtained; such evidence involves the observed evolution of Raman spectra, XPS and FTIR data, change in suspension color, emergence of insulating properties in films, *etc.* In more detail, they are discussed below. (2) Experimentally, a considerable reduction (reaching one–two orders of magnitude) of lateral and vertical sizes of suspension flakes treated in an aqueous solution of HF was revealed. Using the original fluorination process, thin (down to 20 nm), really uniform insulating films with a surface relief of $\sim$2 nm were obtained from a graphene suspension. (3) The dielectric constant of the films (1.1–3.2), the breakdown field strength ($\geq 10^6$ V cm^{-1}), the fixed charge in the film, and the density of states at the interface with silicon were evaluated. Fluorination and particle size reduction in the suspension are factors causing the observed changes in the properties of the obtained films. On the basis of the obtained direct and indirect data on the fluorination reaction proceeding between the HF-containing solution and graphene suspension particles, a model for the suspension fluorination process was proposed, and other processes occurring during the treatment of suspension particles in an aqueous solution of HF were comprehended.

Let us consider in more detail the proofs of graphene suspension fluorination under treatment in an aqueous solution of HF. Generally, oxidation of graphene suspension under HF treatment was assumed, and both variants (oxidation and fluorination) are considered. Nevertheless, evidence for only fluorination was found. (1) The dielectric constant of the layers formed from suspension after a long HF treatment was found to be equal to 1.1. It is exactly the same value of the dielectric constant that was found in ref. 31 for fluorographene. Graphene oxide (GO) has a higher dielectric constant (4.3[37]) and GO fillers are typically used for the formation of GO–polymer composites with a high dielectric constant.[38] (2) As was mentioned above, the temperature stability of the films formed from the HF treated suspension was tested. It is well known that GO film resistivity is generally decreased starting with 100–200 °C, whereas a decrease in FG film resistivity is observed at 400–450 °C.[18] We have observed a decrease in the film resistivity at temperatures 400–450 °C with 2.0 eV activated energy for HF-treated graphene or few-layer graphene samples (CVD, or mechanical exfoliation).[11] For the films obtained from HF-treated suspension, isochronal annealing, again, demonstrates the stability of the properties up to 350 °C. So, oxidation was not found from annealing experiments. (3) The colour of suspension after HF treatment changes from black to white (or more exactly to transparent), and not to brown, as typical for GO. (4) Raman measurements also prove that fluorination rather than oxidation occurs because all peaks completely vanished in the spectra. (5) XPS spectra show the appearance of the F 1s peak at the energy of 687.7 eV for the films from HF-treated suspensions. Such a position of the peak corresponds to sp^3 hybridized chemically bound fluorine ions.[16,17,24] Additional peaks near C 1s also correspond to C–CF, C–CF_2 and C–F bonds[5,7,27] These peaks differed from the position of the peaks in graphene oxide: C–O (286.2 eV), C═O (287.8 eV), and C–OH.[27,39,40] It is worth mentioning here that in our case of treatment in the aqueous solution of HF there are no peaks which correspond to C–F2 and C–F3 typical for fluorination in the gas phase.[5,7,18,27]

In the course of intercalation, the DMF dissolver penetrated in between flake layers, turning the flakes into layered structures. It is known that DMF does not interact chemically with graphene monolayers. An analysis by XPS proves the absence of nitrogen in the obtained films. The absence of the peak due to nitrogen in the XPS spectra of the examined films confirms the fact that, in those films, in the presence of water DMF decomposes into formic acid (HCOOH) and gaseous formamide ($HN(CH_3)_2$) according to the reaction

$$(CH_3)_2NC(O)H + H_2O \rightarrow HCOOH + HN(CH_3)_2\uparrow + \Delta Q \qquad (2)$$

The DMF decomposition reaction proceeding in the presence of water and HF is accompanied by the evolution of heat (342.8 kJ mol^{-1}, or 3.5 eV per each single reaction event).[41] Expectedly, the evolved heat promotes the fluorination reaction according to the previously examined dependence of the rate of graphene and few-layer graphene fluorination on solution temperature.[11] Fluorination and the mismatch between graphene and fluorographene lattice constants (about 1%) lead to the generation of mechanical stress in the layers.[18] Relaxation of mechanical stress results in deformation of fluorinated graphene

layers and the neighbor graphene regions. Following the deformation of graphene, it becomes more reactive, and its wettability with respect to the HF-containing solution increases.[42,43] The wettability of fluorinated graphene with respect to water is higher in comparison with graphene. Due to the change in the flake surface wettability the penetration of the HF-containing solution into flakes can become accelerated. As a result, fluorination of suspension particles leads to their additional exfoliation. The exfoliation and fractionation of suspension flakes are schematically shown in Fig. 3c. The additional exfoliation makes the film and particle thicknesses decrease with the treatment duration (see Fig. 1–4). Besides, as it follows from Fig. 4a, after a sufficiently long treatment the suspension contains, in addition to relatively coarse flakes sized 100 to 400 nm, fine particles sized 20 to 50 nm. In addition, the influence of fluorination on the properties of the obtained films can be judged considering the results of electrical measurements, which show that films obtained from suspensions treated for more than 25 days start displaying insulating properties brought about by the increased fluorination degree of the material.

It seems that, during the preparation of the suspension, DMF penetrated into 20 to 70 nm thick suspension particles only in between very few layers (typically, in between two–four monolayers). The intercalation was not complete, and it did not necessarily cause the splitting of the material along the intercalated layers. Treatment in hydrofluoric acid promoted the completion of DMF intercalation processes and caused the addition exfoliation of suspension elements. Here, the expected minimal thickness of formed flakes is two–four monolayers; it is the very case that we observed in the experiment. It can be hypothesized that further fluorination will make possible splitting of particles into even thinner flakes. However, the latter reactions are expected to be processes occurring much more slowly in comparison with the exfoliation of the material along the DMF-intercalated layers.

XPS data (C 1s peak decomposition for different samples) allow us to estimate the fluorination degree using the area under the peaks. We have obtained formulas $CF_{0.23}$, $CF_{0.5}$ and $CF_{0.65}$ for 25, 40 and 60 days of HF treatments, respectively. The fluorination degrees of the same films extracted from dielectric constant measurements (Fig. 8b) are higher than those estimated from XPS data. The dielectric constant is the factor by which the electric field between the charges is decreased or increased related to vacuum. The presence of small few layer graphene fillers (with a relatively low aspect ratio) in the fluorinated matrix is found to have a weak effect on permittivity of the whole film. It is worth mentioning again that, in the case of a high aspect ratio of graphene fillers (large graphene flakes), the dielectric constant of the composite had strongly changed already for the 1–2% nanosheet volume fraction.[36] It allows us to assume that relatively large graphene flakes sized 100–400 nm are fractionated by fluorination on small graphene quantum dots.

The processes of chemical fragmentation of carbon materials with sp^2-hybridization are well known which, in particular, were used for obtaining nanoribbons out of carbon tubes.[23,44] The processes of chemical cutting of carbon nanotubes were a result of chemical oxidation of the nanotubes; this oxidation was first initiated at lattice defects and, then, it acted to ''unzip'' the tubes. Presently, similar processes are widely used for synthesizing graphene quantum dots sized 1–5 nm in diameter and exhibiting a strong photoluminescence.[45–47] It was assumed that, in aqueous solutions of various acids, the fractionation of particles in initial suspensions into finer particles was initiated in mechanically stressed regions of graphene sheets with high defect concentrations. Most actively, such processes occur in autoclaves at elevated temperatures ($\sim$200 °C) and pressures.[3,18] We believe that similar processes occurred in the suspensions examined in the present study. As it follows from the high amplitude of the D peak in Raman spectra, the graphite and few-layer graphene particles contained a substantial amount of structural defects (Fig. 6a and b). Those defects could be introduced into the material at any suspension preparation stage, be that the mechanical crushing, the DMF dissolver intercalation, or the ultrasonic treatment. During fluorination, the defects are expected to be initiation sites for the fluorination of suspension flakes and, subsequently, at flake rupture points. It seems that finer suspension particles sized 20 to 50 nm serve analogues of quantum dots in the well-known graphene fractionation processes. In the case treated in the present study, large sizes of such flakes were the consequence of the fact that the reaction was carried out under normal conditions (comparatively low temperature and/or pressure). Simultaneously, the suspension also contained coarse round flakes, close in their sizes (100–400 nm), which were the basic suspension elements. Very probably, a more intricate shape of particles would lead to higher mechanical stress generated at the bent surface regions, which can be considered defects present at the boundary and promote the cutting of fragments from the surface.

The unique properties of the dielectric films obtained from the fluorinated suspension are noteworthy. The value of the fixed charge, $\sim 5 \times 10^{10}$ cm^{-2}, and the density of interface states, $\sim 2 \times 10^{10}$ cm^{-2}, can be regarded as excellent values for a dielectric film. Such values can only be reached in SiO_2 layers, featuring a well-established fabrication technology. All the other known dielectric films, including Si_3N_4, Al_2O_3, HFO_2 *etc.*, yield the charge and interface-state densities of 10^{11}–10^{12} cm^{-2}. So, we have obtained the minimum possible charge density in a film. Besides, the films withstand the high electric field strengths of $(1–3) \times 10^6$ V cm^{-1}. A breakdown field strength of 10^7 V cm^{-1} was obtained for fluorographene films produced from graphene and few-layered graphene in fluorine-containing plasma.[31] The obtained values of the dielectric constant of fluorinated films (ε = 3–2 for the moderate fluorination duration of 25–40 days and ε = 1.1 for the sufficiently long fluorination duration of 60–70 days, and hence, different fluorination degrees) varies from values close to the value of ε for amorphous fluorinated graphite ($\sim$2.1) as determined from similar measurements[48] to the value of 1.1 obtained for the few-layer fluorographene structures.[31]

On the whole, the obtained dielectric films exhibit good structural and electrical properties. Owing to the simple preparation procedure of such films and easiness of their application onto substrates, and also owing to the possibility of obtaining very thin layers, fluorinated graphene films offer

promise for application as dielectric layers in thin-film device structures.

Conclusions

The processes occurring during the interaction of DMF-based graphene suspension with a solution of hydrofluoric acid in water were studied. It was found that, as a result of the interaction, the suspension particles undergo an additional splitting (up to 1–5 monolayers) and size reduction (100–300 nm). Evidence proving the fluorination of suspension flakes during the treatment of the suspension with an aqueous solution of HF in water is based on the evolution of Raman spectra, XPS and FTIR data, change in suspension color, and emergence of insulating film properties. A schematic pattern for the joint action of DMF and HF-containing solution for suspension, flakes resulting in additional exfoliation of graphene sheets and formation of thinner and finer fluorinated graphene particles was proposed.

From the fluorinated suspension, thin (100–20 nm), really uniform insulating films were obtained. The films exhibit a surface relief of $\sim$2 nm height, and they can be applied onto arbitrarily large areas. The dielectric constant of the films was determined to be equal to 3.2 down to 1.1 depending on the fluorination degree of the material. It was shown that films prepared from a fluorinated suspension exhibit high breakdown fields ($>1 \times 10^6$ V cm^{-1}), and they contain low charge densities in the film and at the interface with silicon in metal–dielectric–semiconductor structures, the fixed charge density in the film and the density of interface states being $\sim(1\text{–}5) \times 10^{10}$ cm^{-2}. Such excellent characteristics of the dielectric film (high breakdown electrical field and low densities of charges) make them promising layers for use as insulating elements in thin-film device structures. Moreover, the films from the fluorinated suspension are cheap, practically feasible and easy to produce.

Acknowledgements

This work was supported in part by the Russian Foundation for Basic Research (Grant No. 14-32-50270), Siberian Branch of Russian Academy of Sciences (Project 75) and the Ministry of Science and Education of the Russian Federation.

Notes and references

1 K. S. Novoselov, V. I. Fal'ko, L. Colombo, P. R. Gellert, M. G. Schwab and K. Kim, A roadmap for graphene, *Nature*, 2012, **490**(7419), 18–200.

2 E. Bekyarova, S. Sarkar, S. Niyogi, M. E. Itkis and R. C. Haddon, Advances in the chemical modification of epitaxial graphene, *J. Phys. D: Appl. Phys.*, 2012, **45**, 154009.

3 M. Bacon, S. J. Bradley and T. Nann, Graphene quantum dots, *Part. Part. Syst. Charact.*, 2014, **31**(4), 415–428.

4 P. Sessi, J. R. Guest, M. Bode and N. P. Guisinger, Patterning Graphene at the Nanometer Scale *via* Hydrogen Desorption, *Nano Lett.*, 2009, **9**(12), 4343–4347.

5 J. T. Robinson, J. S. Burgess, C. E. Junkermeier, S. C. Badescu, T. L. Reinecke, F. K. Perkins, M. K. Zalalutdniov, J. W. Baldwin, J. C. Culbertson, P. E. Sheehan and E. S. Snow, Properties of Fluorinated Graphene Films, *Nano Lett.*, 2010, **10**(8), 3001–3005.

6 Md. Z. Hossain, J. E. Johns, K. H. Bevan, H. J. Karmel, Y. T. Liang, S. Yoshimoto, K. Mukai, T. Koitaya, J. Yoshinobu, M. Kawai, A. M. Lear, L. L. Kesmodel, S. L. Tait and M. C. Hersam, Chemically homogeneous and thermally reversible oxidation of epitaxial graphene, *Nat. Chem.*, 2012, **4**(4), 305–309.

7 Z. Wanga, J. Wanga, Z. Li, P. Gong, X. Liu, L. Zhang, J. Ren, H. Wang and S. Yang, Synthesis of fluorinated graphene with tunable degree of fluorination, *Carbon*, 2012, **50**(15), 5403–5410.

8 M. Bruna, B. Massessi, C. Cassiago, A. Battiato, E. Vittone, G. Speranzad and S. Borini, Synthesis and properties of monolayer graphene oxyfluoride, *J. Mater. Chem.*, 2011, **21**(46), 18730–18737.

9 O. Ö. Ekiz, M. Ürel, H. Güner, A. K. Mizrak and A. Dâna, Reversible electrical reduction and oxidation of graphene oxide, *ACS Nano*, 2011, **5**(4), 2475–2482.

10 Y. Yang, G. Lu, Y. Li, Z. Liu and X. Huang, One-step preparation of fluorographene: a highly efficient, low-cost, and large-scale approach of exfoliating fluorographite, *ACS Appl. Mater. Interfaces*, 2013, **5**(24), 13478–13483.

11 N. A. Nebogatikova, I. V. Antonova, V. Ya. Prinz, V. A. Volodin, D. A. Zatsepin, E. Z. Kurmaev, I. S. Zhidkov and S. O. Cholakh, Functionalization of graphene and few-layer graphene films in an hydrofluoric acid aqueous solution, *Nanotechnol. Russ.*, 2014, **9**(1–2), 51–59.

12 N. A. Nebogatikova, I. V. Antonova and V. Ya. Prinz, Functionalization of graphene and few-layer graphene with aqueous solution of hydrofluoric acid, *Phys. E*, 2013, **52**, 106–111.

13 L. Britnell, R. V. Gorbachev, A. K. Geim, L. A. Ponomarenko, A. Mishchenko, M. T. Greenaway, T. M. Fromhold, K. S. Novoselov and L. Eaves, Resonant tunnelling and negative differential conductance in graphene transistors, *Nat. Commun.*, 2013, **4**, 1794.

14 A. N. Sidorov, M. M. Yazdanpanah, R. Jalilian, P. J. Ouseph, R. W. Cohn and G. U. Sumanasekera, Electrostatic deposition of graphene, *Nanotechnology*, 2007, **18**(13), 135301.

15 F. Bonaccorso, A. Lombardo, T. Hasan, Z. Sun, L. Colombo and A. C. Ferrari, Production and processing of graphene and 2d crystals, *Mater. Today*, 2012, **15**(12), 564–589.

16 S. Y. Oh, S. H. Kim, Y. S. Chi and T. J. Kang, Fabrication of oxide-free graphene suspension and transparent thin films using amide solvent and thermal treatment, *Appl. Surf. Sci.*, 2012, **258**(22), 8837–8844.

17 M. Zhou, T. Tian, X. Li, X. Sun, J. Zhang, P. Cui, J. Tang and L. Ch. Qin, Production of graphene by liquid-phase exfoliation of intercalated graphite, *Int. J. Electrochem. Sci.*, 2014, **9**, 810–820.

18 R. R. Nair, W. Ren, R. Jalil, I. Riaz, V. G. Kravets, L. Britnell, P. Blake, F. Schedin, A. S. Mayorov, S. Yuan, M. I. Katsnelson, H. M. Cheng, W. Strupinski, L. G. Bulusheva, A. V. Okotrub, I. V. Grigorieva, A. N. Grigorenko, K. S. Novoselov and A. K. Geim, Fluorographene: a two-dimensional counterpart of Teflon, *Small*, 2010, **6**(24), 2877–2884.

19 N. A. Nebogatikova, I. V. Antonova, V. Ya. Prinz, V. B. Timofeev and S. A. Smagulova, Graphene quantum dots in fluorographene matrix formed by means of chemical functionalization, *Carbon*, 2014, **77**, 1095–1103.

20 S. F. Tayyari, H. Reissi, F. Milani-Nejad and I. S. Butler, Vibrational assignment of α-cyanoacetylacetone, *Vib. Spectrosc.*, 2001, **26**(2), 187–199.

21 S. E. Fisher, J. M. Chalmers, A. Marcelli, H. J. Byrne, F. Lyng, P. Lasch, L. M. Miller, P. Dumas, P. Gardner and D. Moss, *Biomedical Applications of Synchrotron Infrared Microspectroscopy (RSC Analytical Spectroscopy)*, Royal Society of Chemistry, 2010.

22 P. B. Nagabalasubramanian, S. Periandy and S. Mohan, A scaled quantum mechanical approach of vibrational analysis of o-tolunitrile based on FTIR and FT Raman spectra, *ab initio*, Hartree Fock and DFT methods, *Spectrochim. Acta, Part A*, 2009, **74**(5), 1280–1287.

23 V. N. Khabashesku, Covalent functionalization of carbon nanotubes: synthesis, properties and applications of fluorinated derivatives, *Russ. Chem. Rev.*, 2011, **80**, 705–728.

24 S. D. Sherpa, G. Levitin and D. W. Hess, Effect of the polarity of carbon-fluorine bonds on the work function of plasma-fluorinated epitaxial graphene, *Appl. Phys. Lett.*, 2012, **101**, 111602.

25 N. O. Plank, L. Jiang and R. Cheung, Fluorination of carbon nanotubes in CF_4 plasma, *Appl. Phys. Lett.*, 2003, **83**, 2426–2428.

26 G. Tsoukleri, J. Parthenios, K. Papagelis, R. Jalil, A. C. Ferrari, A. K. Geim, K. S. Novoselov and C. Galiotis, Subjecting a graphene monolayer to tension and compression, *Small*, 2009, **5**, 2397–2402.

27 X. Wang, Y. Dai, J. Gao, J. Huang, B. Li, C. Fan, J. Yang and X. Liu, High-Yield Production of Highly Fluorinated Graphene by Direct Heating Fluorination of Graphene-oxide, *ACS Appl. Mater. Interfaces*, 2013, **5**, 8294–8299.

28 F. Karlick, K. Kumara, R. Datta, M. Otyepka and R. Zboril, Halogeneted graphenes: rapidly grown family of graphene deriviatives, *ACS Nano*, 2013, **7**, 64343–64364.

29 P. W. Gong, Z. F. Wang, J. Q. Wang, H. G. Wang, Z. P. Li, Z. J. Fan, Y. Xu, X. X. Han and S. R. Yang, One-pot sonochemical preparation of fluorographene and selective Tunning of its fluorine coverage, *J. Mater. Chem.*, 2012, **22**, 16990–16996.

30 Y. Wang, W. C. Lee, K. K. Manga, P. K. Ang, J. Lu, Y. P. Liu, C. T. Lim and K. P. Loh, Fluorinated graphene for promoting neuro-induction of stem cells, *Adv. Mater.*, 2012, **24**, 4285–4290.

31 K. I. Ho, C. H. Huang, J. H. Liao, W. Zhang, L. J. Li, C. S. Lai and C. Y. Su, Fluorinated Graphene as High Performance Dielectric Materials and the Applications for Graphene Nanoelectronics, *Sci. Rep.*, 2014, **4**, 5893.

32 Z.-M. Dang, J.-K. Yuan, J.-W. Zha, T. Zhou, S.-T. Li and G.-H. Hu, Fundamentals, processes and applications of high-permittivity polymer-matrix composites, *Prog. Mater. Sci.*, 2012, **57**, 660–723.

33 D. A. G. Bruggeman, The calculation of various physical constants of heterogeneous substances. I. The dielectric constants and conductivities of mixtures composed of isotropic substances, *Ann. Phys.*, 1935, **24**, 636–642.

34 C. W. Nan, Comment on 'Effective dielectric function of a random medium', *Phys. Rev. B: Condens. Matter Mater. Phys.*, 2001, **63**, 176201.

35 Z.-M. Dang, J.-K. Yuan, S.-H. Yao and R.-J. Liao, Flexible nanodielectric materials with high permittivity for power energy storage, *Adv. Mater.*, 2013, **25**(44), 6334–6365.

36 D. Wang, T. Zhou, J.-W. Zha and Z.-M. Dang, Functionalized graphene – $BaTiO_3$/ferroelectric polymer nanodielectric composites with high permittivity, low dielectric loss, and low percolation threshold, *J. Mater. Chem. A*, 2013, **1**, 6162–6168.

37 B. Standley, A. Mendez, E. Schmidgall and M. Bockrath, Graphene–Graphite Oxide Field-Effect Transistors, *Nano Lett.*, 2012, **12**, 1165–1169.

38 J.-Y. Kim, J. Lee, W. H. Lee, I. N. Kholmanov, J. W. Suk, T. Y. Kim, Y. Hao, H. Chou, D. Akinwande and R. S. Ruoff, Flexible and Transparent Dielectric Film with a High Dielectric Constant Using Chemical Vapor Deposition-Grown Graphene Interlayer, *ACS Nano*, 2014, **8**, 269–274.

39 S. Mao, K. Yu, S. Cui, Z. Bo, G. Lu and J. Chen, A new reducing agent to prepare single-layer, high-quality reduced graphene oxide for device applications, *Nanoscale*, 2011, **3**, 2849–2853.

40 V. H. Pham, H. D. Pham, T. T. Dang, S. H. Hur, E. J. Kim, B. S. Kong, S. Kima and J. S. Chung, Chemical reduction of an aqueous suspension of graphene oxide by nascent hydrogen, *J. Mater. Chem.*, 2012, **22**, 10530–10536.

41 P. W. Atkins and P. J. De. Atkins, *Physical chemistry*, Oxford University Press, Oxford, 2006.

42 W. Xiong, J. Z. Liu, Zh. L. Zhang and Q. S. Zhen, Control of surface wettability *via* strain engineering, *Acta Mech. Sin.*, 2013, **29**(4), 543–549.

43 D. W. Boukhvalov and M. I. Katsnelson, Chemical functionalization of graphene, *J. Phys.: Condens. Matter*, 2009, **21**(34), 344205.

44 Z. Gu, H. Peng, R. H. Hauge, R. E. Smalley and J. L. Margrave, Cutting single-wall carbon nanotubes through fluorination, *Nano Lett.*, 2002, **2**(9), 1009–1013.

45 Z. Chen, T. Huang, B. C. Jin, J. Hu, H. Lu and S. Nutt, High yield synthesis of single-layer graphene microsheets with dimensional control, *Carbon*, 2014, **68**, 164–174.

46 H. Tetsuka, R. Asahi, A. Nagoya, K. Okamoto, I. Tajima, R. Ohta and A. Okamoto, Optically tunable amino-functionalized graphene quantum dots, *Adv. Mater.*, 2012, **24**(39), 5333–5338.

47 M. Xu, Z. Li, X. Zhu, N. Hu, H. Wei, Z. Yang and Y. Zhang, Hydrothermal/solvothermal synthesis of graphene quantum dots and their biological applications, *Nano Biomed. Eng.*, 2013, **5**(2), 65–71.

48 Y. Ma, H. Yang, J. Guo, C. Sathe, A. Agui and J. Nordgren, Structural and electronic properties of low dielectric constant fluorinated amorphous carbon films, *Appl. Phys. Lett.*, 1998, **72**, 3353–3355.

